# Structure of Human Histocompatibility Leukocyte Antigen (HLA)-Cw4, a Ligand for the KIR2D Natural Killer Cell Inhibitory Receptor

By Qing R. Fan and Don C. Wiley

*From the Department of Molecular and Cellular Biology, Howard Hughes Medical Institute, Harvard University, Cambridge, Massachusetts 02138*

## Summary

The crystal structure of the human class I major histocompatibility complex molecule, human histocompatibility leukocyte antigen (HLA)-Cw4, the ligand for a natural killer (NK) cell inhibitory receptor, has been determined, complexed with a nonameric consensus peptide (QYDDAVYKL). Relative to HLA-A2, the peptide binding groove is widened around the COOH terminus of the α1 helix, which contains residues that determine the specificity of HLA-Cw4 for the inhibitory NK receptor, KIR2D. The structure reveals an unusual pattern of internal hydrogen bonding among peptide residues. The peptide is anchored in four specificity pockets in the cleft and secured by extensive hydrogen bonds between the peptide main chain and the cleft. The surface of HLA-Cw4 has electrostatic complementarity to the surface of the NK cell inhibitory receptor KIR2D.

Key words: HLA-Cw4 • crystal structure • killer cell inhibitory receptor • natural killer cell recognition • autoimmunity

Class I MHC molecules in both humans and mice mediate target cell recognition by CTLs and NK cells. In humans, class I MHC heavy chains are encoded by three gene loci, HLA-A, -B, and -C. HLA-A and -B molecules are expressed abundantly on the cell surface; they are primarily responsible for presenting viral or tumor antigens to $CD8^+$ CTLs. Structures of HLA-A and -B molecules bound to a single peptide or a mixture of peptides have demonstrated that the sequence and conformation of the peptide largely determines the antigenic identity of the peptide–MHC complex (for review see references 1 and 2). HLA-C is expressed at much lower levels on the cell surface and presents antigens less efficiently than HLA-A and -B (3). Although an HLA-Cw4–restricted CTL clone that recognizes a highly conserved region of human HIV-1 gp120 (4) and a $CD8^+$ HIV-1 gag-specific T lymphocyte clone that is restricted by HLA-Cw3 (5) have been described, HLA-C molecules are more restricted in their peptide binding than HLA-A and -B alleles (6). HLA-C alleles are associated with susceptibility to autoimmune diseases (3); increased frequency of HLA-Cw4, for example, correlates with the occurrence of type 2 diabetes (7). HLA-Cw4 is also associated with the rapid progression of AIDS (8). One of the major functions of HLA-C molecules lies in NK cell recognition.

Human inhibitory NK cell receptors specifically recognize class I MHC molecules on target cell surfaces and deliver an inhibitory signal that prevents target cell lysis by NK cells (for review see references 9 and 10). Killer cell Ig-like receptors (KIRs)[1] on NK cells have been identified for polymorphic HLA-B and -C molecules (11–13). KIR2D molecules (KIRs with two Ig-like domains, also referred to as p58 and p50) are involved in the recognition of HLA-C and distinguish the polymorphism at positions 77 and 80 of the HLA-C heavy chain (14). HLA-Cw4 and related alleles (HLA-Cw2, -Cw5, and -Cw6) have Asn77 and Lys80 and are recognized by KIR reactive with the EB6 (15) or HP-3E4 (16) antibody (e.g., KIR2DL1). HLA-Cw3 and related alleles (HLA-Cw1, -Cw7, and -Cw8) contain Ser77 and Asn80 and interact with KIR that are reactive with the GL183 antibody (15) (e.g, KIR2DL2). The structure of the HLA-Cw4–specific KIR2DL1 (originally named p58-cl42 KIR) has been recently determined (17); it consists of two Ig-like domains positioned at an acute 60° angle. Residues at the domain elbow of KIR2DL1 have been identified as important for HLA-Cw4 binding (18–20).

In this study, we present the structure of HLA-Cw4 (Cw*0401; Protein Data Bank accession code 1QQD), which specifically interacts with KIR2DL1. The conformation of the nonameric peptide bound to HLA-Cw4 is stabilized by the internal hydrogen bonding among peptide resi-

[1]*Abbreviations used in this paper:* KIRs, killer cell Ig-like receptors; PEG, polyethylene glycol; rms, root mean square.

dues. The peptide side chains fit into four specificity pockets, and extensive hydrogen bonds form between peptide main chain atoms and the MHC heavy chain along the peptide. Relative to HLA-A2, the peptide binding groove of HLA-Cw4 is widened at the COOH-terminal portion of the α1 helix (up to 2.4 Å), and the adjacent loop region (residues A14–20) protrudes up and toward the α1 helix (up to 4.2 Å). The COOH terminus of the α1 helix forms a potential KIR binding site on HLA-Cw4 and is analyzed in light of the receptor and peptide–MHC ligand structures.

## Materials and Methods

*Protein Purification and Crystallization.* The HLA-Cw4 heavy chain (residues A1–275) was overexpressed in the *Escherichia coli* strain BL21 (DE3) pLysS and purified as insoluble inclusion body protein (21). $\beta_2$m (microglobulin) inclusion body was produced in the *E. coli* strain XA90 as described (22). The HLA-Cw4 heavy chain and $\beta_2$m were reconstituted in the presence of the peptide, QYDDAVYKL, and the refolded complex was purified by gel filtration chromatography (21). Refolded HLA-Cw4 crystallized in 18% polyethylene glycol (PEG) 8000, 0.2 M Ca acetate, and 0.1 M Na cacodylate, pH 6.5. The crystals obtained initially were thin plates and were improved by streak seeding using 12% PEG 8000, 0.2 M Ca acetate, and 0.1 M Na cacodylate, pH 6.5, as the reservoir solution. The space group is $P2_12_12_1$, with one molecule per asymmetric unit, and unit cell parameters a = 54.96 Å, b = 77.49 Å, and c = 108.59 Å.

*Data Collection.* The crystals were stabilized in a harvesting solution (22.5% PEG 8000, 0.2 M Ca acetate, and 0.1 M Na cacodylate, pH 6.5) for 2 h and then soaked in a cryoprotectant-containing solution (22.5% PEG 8000, 0.2 M Ca acetate, 0.1 M Na cacodylate, pH 6.5, and 25% glycerol) for 5 min before being flash-cooled with liquid nitrogen. X-ray diffraction data were collected to 2.9 Å with the ADSC 1K CCD detector at A-1 beamline of the Cornell High Energy Synchrotron Source (CHESS; Ithaca, NY). The diffraction was anisotropic, and the mosaicity of the crystal varied from 0.5 to 1.5° depending on the orientation of the crystal. Data were integrated and scaled (Table I) using DENZO and SCALEPACK (HKL Research).

*Molecular Replacement and Refinement.* The HLA-Cw4 structure was determined by molecular replacement using the program AMoRe (23). Except for the peptide, the HLA-B27 molecule (Protein Data Bank [Brookhaven National Laboratory, Upton, NY] accession code 1HSA; reference 24) was used as the search model. Rotation and translation function searches using all data from 8 to 4 Å yielded a clear solution with a correlation coefficient of 44.9% and R factor of 44.4% (the next highest peak has a correlation coefficient of 26.7% and R factor of 51.0%).

The molecular replacement solution was used as the starting model for refinement, with residues that differ between HLA-Cw4 and HLA-B27 (34 total residues in the heavy chain) replaced by alanines and the peptide excluded. All data from 22 to 2.9 Å, with $|Fo| > 0$, were included for refinement; 10% of the reflections were omitted for the calculation of $R_{free}$. The model was subjected to an initial rigid body refinement in X-PLOR (25), where α1α2, α3, and $\beta_2$m were treated as individual domains. After two rounds of manual rebuilding in O (26) and refinement in X-PLOR, which involved simulated annealing with bulk solvent correction, clear electron density appeared in the 3Fo-2Fc map for the peptide region, including all of the side chains of the peptide. Subsequent refinement used the maximum likelihood method implemented in crystallography and nuclear magnetic resonance system (CNS) (27). The minimization procedure included positional refinement and simulated annealing with bulk solvent correction and initial overall anisotropic B factor correction, followed by group B factor refinement. The final model contains residues A2–274 of the heavy chain, B0–98 of $\beta_2$m (B0 corresponds to the initial methionine that was engineered for expression in *E. coli*), P1–9 of the peptide, and 35 water molecules (Table I). The 35 water molecules were selected and refined based on peaks that were at least 2.0 σ in height in Fo-Fc and 3Fo-2Fc electron density maps. All φ and ψ angles lie in the allowed regions of the Ramachandran plot, with 86% in the most favorable regions. The $NH_2$ and COOH termini of the heavy chain (A1 and A275), as well as the COOH terminus of $\beta_2$m (B99), have no visible electron density. Side chains for residues A104–108 and A195–198 in the loop region of the heavy chain and residues B17–19 of $\beta_2$m have weak electron densities and B factors >80 Å$^2$.

**Table I.** *Statistics for Data Collection and Refinement*

| Data collection | | |
|---|---|---|
| Resolution (Å) | 22–2.9 | 3.0–2.9 |
| Unique reflections | 10,533 | 995 |
| Unique reflections (>3 σ) | 9,849 | 804 |
| Completeness (%) | 97.9 | 96.9 |
| Redundancy | 5 | 4 |
| $R_{sym}$ (%)* | 11.2 | 32.3 |
| **Refinement (22–2.9 Å)** | | |
| No. reflections | 9,448 | |
| No. reflections ($R_{free}$ set)§ | 1,085 | |
| $R_{cryst}$ (%)‡ | 21.6 | |
| $R_{free}$ (%)§ | 27.1 | |
| Nonhydrogen protein atoms | 3,144 | |
| Water molecules | 35 | |
| Average B factors (Å$^2$) | 49.7 | |
| Root mean square deviations | | |
| Bonds (Å) | 0.008 | |
| Angles (°) | 1.70 | |
| B factors (Å$^2$) | 2.5 | |
| Estimated coordinate error (Å)‖ | 0.33 | |
| Ramachandran plot statistics (%) | | |
| Residues in most favored regions | 85.8 | |
| Residues in additional allowed regions | 13.0 | |
| Residues in generously allowed regions | 1.2 | |
| Residues in disallowed regions | 0.0 | |

*$R_{sym} = (\Sigma|I(i) - <I>|)/(\Sigma I(i))$, where $I(i)$ is the intensity of an individual reflection and $<I>$ is the average intensity of that reflection.
‡$R_{cryst} = (\Sigma||Fo| - |Fc||)/(\Sigma|Fo|)$, where Fo and Fc are the observed and calculated structure factor amplitudes.
§$R_{free}$ is equivalent to $R_{cryst}$ but calculated for a randomly chosen 10% of reflections that were omitted from the refinement process.
‖Coordinate error is estimated from the Luzzati plot in CNS (70).

## Results

*Overall Structure of the Consensus Peptide–HLA-Cw4 Complex*. The ectodomain of the HLA-Cw4 heavy chain was overexpressed as inclusion bodies in *E. coli* and reconstituted in the presence of $\beta_2$m and a nonameric peptide (QYDDAVYKL) that contains the consensus peptide binding motif for HLA-Cw4 (21, 28, 29). The consensus peptide motif was determined by pool sequencing and included an aromatic residue or proline for P2, a hydrophobic COOH-terminal anchor, a hydrophobic auxiliary anchor at P6, and the frequent use of glutamic acid and aspartic acid at P4 (29). Refolded HLA-Cw4 binds directly to KIR2DL1, as shown by a native gel shift assay (21). The crystal structure of HLA-Cw4 was determined by molecular replacement, using HLA-B27 (24) as the search model, and refined at 2.9 Å ($R_{cryst}$ = 21.6%; $R_{free}$ = 27.1%). The final model contains heavy chain residues A2–274, $\beta_2$m residues B0–98, peptide residues P1–9, and 35 water molecules. The loop regions at residues A104–108 and A195–198 in the heavy chain and residues B17–19 in $\beta_2$m have weak electron density and high B factors (>80 Å$^2$), indicating that these regions are disordered. Clear electron density is observed for the entire peptide (Fig. 1).

The overall structure of HLA-Cw4 is similar to that of HLA-A and -B molecules (24, 30–34), as expected from the high sequence homology (~85% sequence identity) among HLA-A, -B, and -C heavy chains. The root mean square (rms) deviation between HLA-Cw4 and HLA-A2 is 0.8 Å for 368 $C_\alpha$ atoms, and the rms between HLA-Cw4 and B53 is 0.8 Å for 380 $C_\alpha$ atoms. (HLA-A2 [2.5 Å] and -B53 [2.3 Å] are chosen for comparison because the structures of these molecules bound to single nonameric peptides are available at high resolution.) The structure differences among HLA-A, -B, and -C molecules are due to the relative orientations of the individual $\alpha1\alpha2$, $\alpha3$, and $\beta_2$m domains. The $\alpha1\alpha2$ domains of HLA-Cw4 and HLA-A2 can be superimposed with an rms deviation of only 0.6 Å for 172 $C_\alpha$ atoms. As shown in Fig. 2 a, when the $\alpha1\alpha2$ domains of HLA-Cw4 and HLA-A2 are superimposed, the $\alpha3$ domain adopts a different position relative to $\alpha1\alpha2$ in each structure.

In the $\alpha1\alpha2$ domain, the structure of HLA-Cw4 differs from many human and mouse class I MHC structures near the COOH-terminal portion of the $\alpha1$ helix (residues A67–77), widening the peptide binding groove in this region by up to 2.4 Å in comparison with HLA-A2 (reference 32; Fig. 2 b). HLA-Cw4 also differs dramatically (up to 4.2-Å shift in $C_\alpha$ atom positions) from HLA-A2 in the loop region connecting S1 and S2 of the $\alpha1$ domain $\beta$ sheet (residues A14–20) (Fig. 2 b). Relative to HLA-A2, the S1-S2 loop protrudes up and toward the $\alpha1$ helix (Fig. 2 a). As a result, Arg17 in HLA-Cw4 partially replaces Arg14 found in HLA-A2 in forming a hydrogen bond with Glu19 and a salt bridge to Asp39 (not shown). Furthermore, two salt bridges between Glu19 in the loop and Arg75 on the $\alpha1$ helix are lost. As the S1-S2 loop is involved in crystal packing and may be an artifact, the biological significance of the loop difference remains to be explored. Other regions in the $\alpha1\alpha2$ domain that differ between HLA-Cw4 and HLA-A2 include the loop connecting S3 and S4 of the $\alpha1$ domain $\beta$ sheet (residues A38–45, up to 2.8-Å difference in $C_\alpha$ positions) (Fig. 2 b). The COOH-terminal end of the $\alpha1$ helix is implicated in HLA-C recognition by KIR (for review see references 9 and 10). The $\alpha2$ helix has been observed to affect binding of Ly-49 to mouse class I MHC molecules (35–37). It is unknown whether the $\alpha2$ helix may also participate in the KIR–HLA-C interaction. The COOH-terminal end of the $\alpha1$ helix, together with its adjacent loop region, may define a KIR binding site on HLA-C that is different from the Ly-49 binding site on mouse class I MHC molecules.

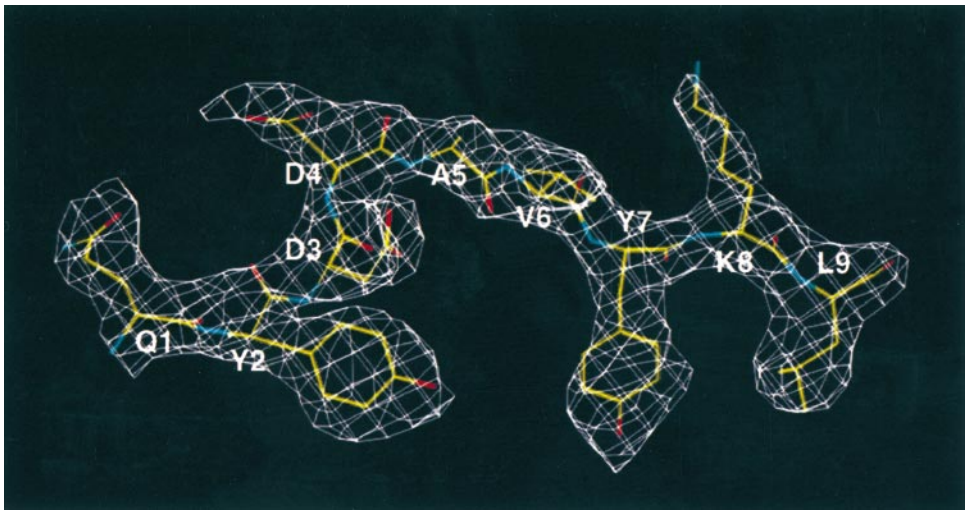


**Figure 1.** 2Fo-Fc simulated annealing omit electron density map of HLA-Cw4 contoured at 1.0 $\sigma$ and in the region of the peptide (displayed in O with a map cover radius of 1.0 Å) (26). Peptide residues and positions are labeled, QYDDAVYKL.

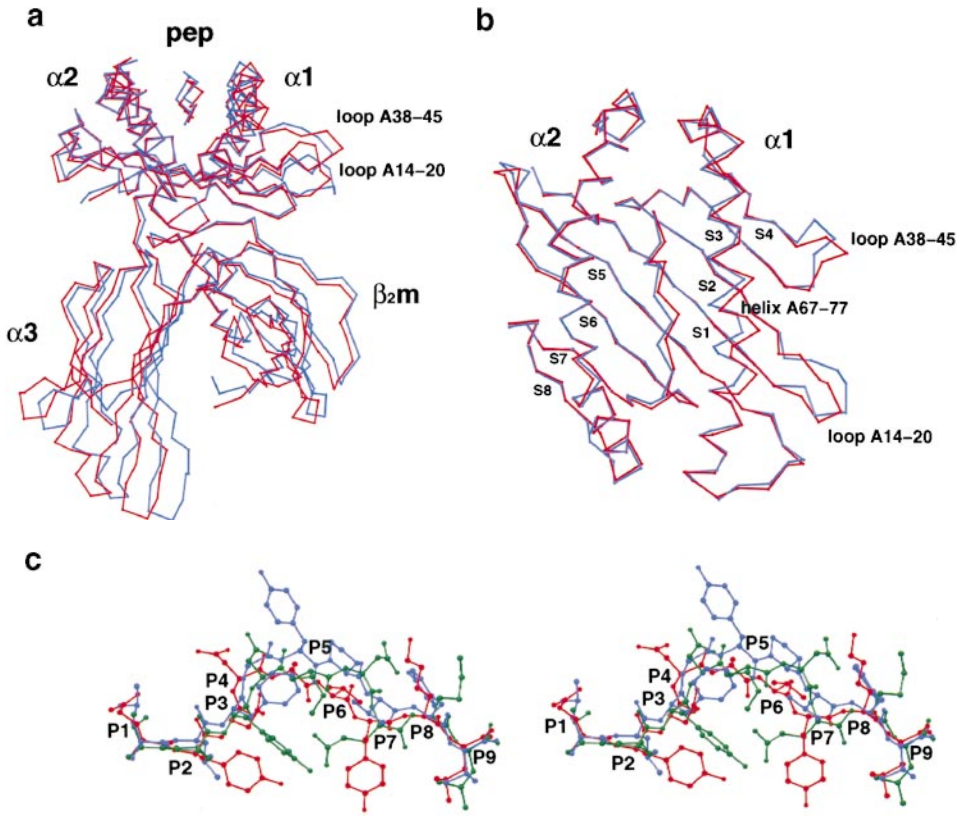


**Figure 2.** (a) Cα traces of HLA-Cw4 (red) and HLA-A2 (blue) (RIBBONS; reference 69). The α1α2 domains of the two structures have been superimposed. The positions of the α3 and $\beta_2$m domains vary in each structure. (b) Top view of the superimposed α1α2 domains of HLA-Cw4 (red) and HLA-A2 (blue). HLA-Cw4 and HLA-A2 differ significantly at the COOH-terminal end of the α1 helix (A67–77) and in the adjacent loop regions (A14–20 and A38–45). The eight β strands are marked S1–S8. (c) Stereo view of the superposition of the peptides bound to HLA-Cw4 (QYDDAVYKL, red), HLA-A2 (Tax peptide, LLFGYPVYV, blue) and HLA-B53 (gag peptide from HIV2, TPYDINQML, green). The peptides are brought into superposition by superimposing the α1α2 domains of the HLA-Cw4, -A2, and -B53 heavy chains. The peptides are viewed from the side as they lie in the peptide binding groove.

The α3 and $\beta_2$m domains of HLA-Cw4 are very similar to those of HLA-A2. One of the regions that varies among the different HLA molecules in the α3 domain is the loop consisting of the acidic residues A223–229. Similar to other class I MHC molecules, residues A225–227 in HLA-Cw4 form a turn of $3_{10}$ helix. The loop is involved in the binding of CD8 to class I MHC (38).

*Extensive Peptide–HLA-Cw4 Interactions along the Peptide Result in Large Buried Surface Area.* Structures of HLA-A and -B have demonstrated that the ends of the peptides (P1–P2, P8–P9) are similarly bound in the cleft through conserved hydrogen bonds, whereas the structural variations occur in the central portion of the peptides. Fig. 2 c compares the conformation of peptides bound to HLA-Cw4 (QYDDAVYKL), HLA-A2 (Tax peptide, LLFGYPVYV; reference 32), and HLA-B53 (epitope gag peptide from HIV2, TPYDINQML; reference 33). As in other HLA structures, the peptide termini in HLA-Cw4 are anchored in the cleft by a number of contacts between the peptide main chain atoms and conserved MHC side chains (Table II; Fig. 3 a). At the $NH_2$ terminus, the P1Gln main chain atoms hydrogen-bond to three tyrosine residues from HLA-Cw4 (Tyr7, 159, and 171). A hydrogen bond between the main chain $NH_2$ group of P2Tyr and the side chain carboxylate of Glu63, which is observed in HLA-A2 and -B27 but absent in HLA-B53, is found in the HLA-Cw4 structure. The conserved hydrogen bonds at the COOH terminus include the ones from the terminal carboxylate oxygen of P9Leu to the side chains of Thr143 and Lys146. The invariant hydrogen bond from the carbonyl oxygen at P8Lys to the pyrrole nitrogen of Trp147 is also present. In addition to the conserved hydrogen bonding network found at the peptide termini, extensive interactions also occur between HLA-Cw4 and the central portion of the peptide. For peptide residues P2–P8, there are five hydrogen bonds from the peptide main chain to HLA-Cw4 side chain atoms and two from the peptide side chain to HLA-Cw4 side chain atoms. We have not been able to observe any water molecule in the region of the peptide, probably due to the limitation of the resolution.

The solvent-accessible surface area buried upon peptide binding for HLA-Cw4 is greater than that found in most peptide–MHC complexes. In the case of HLA-A2 bound to the Tax peptide (LLFGYPVYV), the total solvent-accessible area buried is 1,723 Å$^2$ (calculated using the program SURFACE, reference 39; probe radius, 1.4 Å); for HLA-B53 bound to the gag epitope of HIV2 (TPYDINQML), the area buried is 1,647 Å$^2$. In contrast, a total 1,914 Å$^2$ of solvent-accessible surface area is buried (1,109 Å$^2$ on the peptide and 805 Å$^2$ on the MHC heavy chain) upon peptide binding to HLA-Cw4. As shown by the plot in Fig. 4, the three $NH_2$-terminal residues (P1–P3) and the COOH-terminal residue (P9) of the HLA-Cw4 peptide are almost completely buried (with >93% of the surface area buried for each residue). The two residues in the central region that are mostly exposed are P4Asp and P8Lys. P4Asp is the highest point of the peptide; together, P4Asp and P3Asp form the kink in the peptide main chain conformation that has been

**Table II.** *Peptide Hydrogen Bonds to HLA-Cw4*

| Peptide | | Hydrogen bond partner | | |
|---|---|---|---|---|
| Residue | Atom | Residue | Atom | Distance |
| | | | | *Å* |
| P1Gln | N | Tyr7 | OH | 3.0 |
| | N | Tyr171 | OH | 2.8 |
| | Nε2 | Glu63 | Oε1 | 3.1 |
| | Oε1 | Lys66 | Nζ | 2.9 |
| | O | Tyr159 | OH | 2.6 |
| P2Tyr | N | Glu63 | Oε2 | 2.7 |
| | O | Lys66 | Nζ | 3.0 |
| | O | P4Asp* | N | 3.2 |
| P3Asp | Oδ1 | P4Asp* | N | 3.1 |
| | Oδ1 | P5Ala* | N | 2.9 |
| | Oδ2 | Arg156 | N | 3.0 |
| P5Ala | O | Arg156 | Nη1 | 3.2 |
| P6Val | O | Arg156 | Nη2 | 3.2 |
| P7Tyr | OH | Asp74 | Oδ1 | 3.1 |
| | OH | Asp74 | Oδ2 | 2.9 |
| P8Lys | O | Trp147 | Nε1 | 2.8 |
| P9Leu | N | Asn77 | Oδ1 | 2.8 |
| | O | Lys146 | Nζ | 3.2 |
| | O | Thr143 | Oγ1 | 3.1 |

Hydrogen bonds (<3.2 Å, generated in O; reference 1) from peptide residues QYDDAVYKL to HLA-Cw4.
*Internal hydrogen bonds between peptide residues. All other residues that form hydrogen bonds with the peptide belong to the HLA-Cw4 heavy chain.

observed for many known structures of peptides bound to class I MHC molecules. P8Lys, on the other hand, has been implicated in the binding of HLA-Cw4 to KIR (40).

*Internal Hydrogen Bonding of Peptide Stabilizes the Conformation of the HLA-Cw4–Bound Peptide*. The HLA-Cw4 structure differs from most known structures of class I MHC molecules in that the peptide conformation includes a pattern of internal hydrogen bonding within the peptide (Fig. 3 b). The main chain–main chain hydrogen bond between the carbonyl oxygen of P2Tyr and the $NH_2$ group of P4Asp causes P4Asp to adopt $\phi$ and $\psi$ angles that are found in a left-handed helix and usually observed in residues forming tight turns and kinks ($\phi = 73.8°$, $\psi = 18.2°$). All other residues of the peptide have $\phi$ and $\psi$ angles that are typical for an extended $\beta$ strand. In addition, two hydrogen bonds are also formed between a side chain carboxylate oxygen atom of P3Asp and the main chain amino groups of P4Asp and P5Ala. The side chain of P3Asp can not fit into a small D pocket (41) underneath the $\alpha 2$ helix and formed by the side chains of Arg97, Phe99, Arg156, and Tyr159 (Fig. 5 c). As a result, although the $C_\beta$ atom of P3Asp points toward the $\alpha 2$ helix, its side chain carboxylate is turned back toward the peptide, forming hydrogen bonds with the peptide main chain atoms and the side chain atoms of Arg156 (Fig. 3 b; Table II). An internal hydrogen-bonded type I turn has previously been identified in the structure of an HIV gp120 peptide bound to murine H-2D$^d$ (42, 43).

P3Asp and P4Asp are important for the binding of the consensus peptide to HLA-Cw4. A peptide containing a single amino acid substitution from P3Asp→P3Ala fails to increase the level of assembled HLA-Cw4 on the surface of the TAP-deficient RMA-S cells that are transfected with the HLA-Cw4 cDNA and human $\beta_2$m (40). The P3Asp→P3Ala mutation results in the loss of three hydrogen bonds mediated by the P3Asp side chain, two internal hydrogen bonds and one hydrogen bond with the side chain of Arg156. Substituting P3Asp and P4Asp with P3His and P4Pro also abolishes peptide binding to the cleft (40). These substitutions would have eliminated all of the internal hydrogen bonds that stabilize the peptide conformation. The side chain of P3His would not be able to fit into the small D pocket, which remains unoccupied even in the case of a smaller side chain of P3Asp. Furthermore, electronic repulsion between the side chains of Arg97, Arg156, and P3His would have greatly destabilized the peptide–MHC complex.

*Four Specificity Pockets Explain the Sequence Motif of HLA-Cw4–specific Peptides*. The HLA-Cw4 peptide binding groove is characterized by four specificity pockets (Fig. 5, a and b). The P1 pocket forms the $NH_2$-terminal boundary of the peptide binding groove and is located in the region of the A pocket (41). The peptide binding groove is completely blocked at this end by the residues Arg62 and Trp167, which point toward each other across the cleft (not shown). The P1 pocket includes the highly conserved tyrosine residues 7, 159, and 171, which hydrogen-bond to the peptide $NH_2$ terminus (Fig. 3 a). As in HLA-A2, the pocket is lined with the rather polar residues Tyr59, Glu63, Lys66, Tyr159, Thr163, Cys164, and Tyr171, and its floor is formed by Met5 and Tyr7. The P1Gln side chain is firmly positioned by two hydrogen bonds from its side chain amide group to Glu63 and Lys66. Substitution of P1Gln by P1Ser induces a similar level of HLA-Cw4 expression on the cell surface (40), indicating that the P1 pocket is accommodating to medium sized polar residues.

The HLA-Cw4 structure possesses a P2 pocket that is highly specific for tyrosine. The P2 pocket is formed by a cluster of aromatic residues, including Tyr7, Phe22, Tyr67, and Phe99. The hydroxyl group of P2Tyr points toward two polar residues, Arg97 and Gln70, which separate the P2 pocket from the neighboring P7 pocket. The P2 pocket is rather spacious and is not completely filled even by the bulky side chain of P2Tyr. It is conceivable that with minor adjustments, a water molecule could bridge the interaction between the hydroxyl group of P2Tyr and the polar side chains of Arg97 and Gln70. The role of water molecules in mediating the interaction between the peptide and the cleft has been observed in the structures of both human and mouse class I MHC molecules, including HLA-B53, HLA-B27, H-2K$^b$, H-2D$^b$, H-2D$^d$, and H2-M3 (24, 33, 42, 44–46).

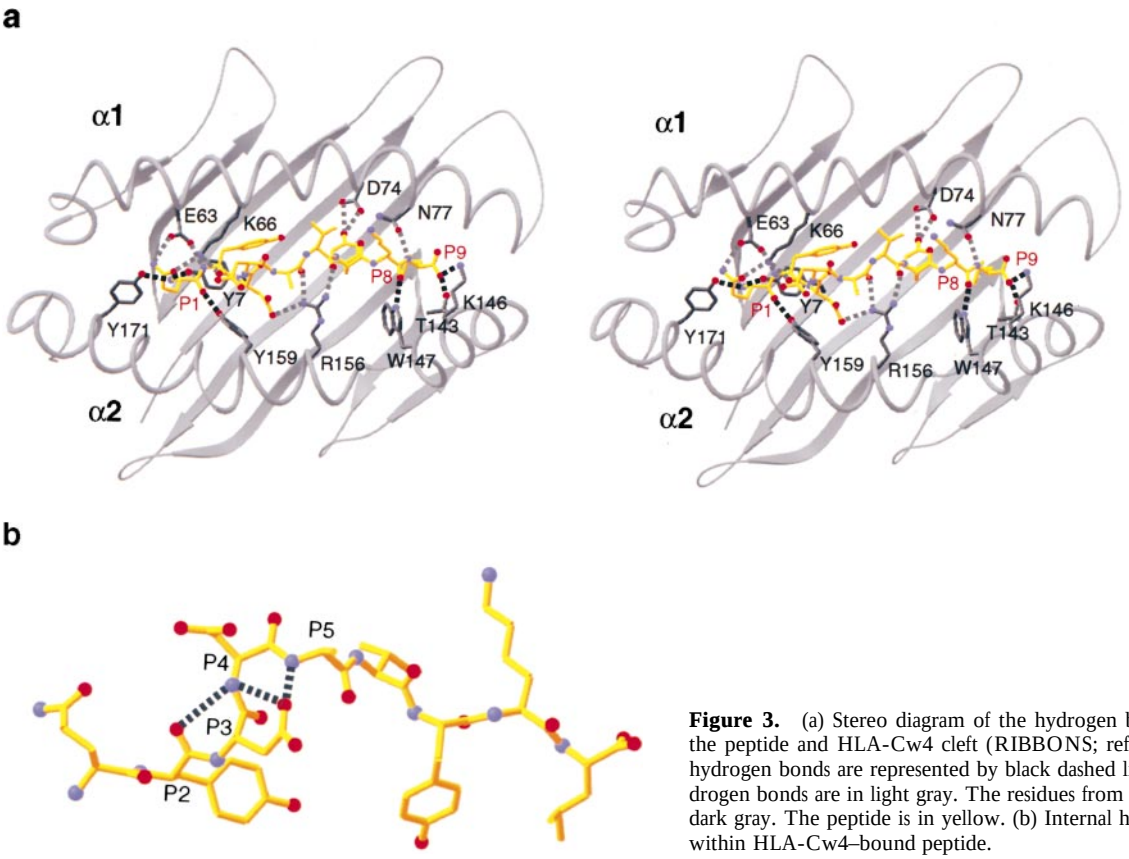


**Figure 3.** (a) Stereo diagram of the hydrogen bonds formed between the peptide and HLA-Cw4 cleft (RIBBONS; reference 69). Conserved hydrogen bonds are represented by black dashed lines, and the other hydrogen bonds are in light gray. The residues from HLA-Cw4 are colored dark gray. The peptide is in yellow. (b) Internal hydrogen bonds formed within HLA-Cw4–bound peptide.

Proline was identified by pool sequencing to be an alternative anchor residue at P2 for HLA-Cw4 (29). Cellular binding assays indicate that substitution of P2Tyr with P2Pro abolishes peptide binding to cell-surface HLA-Cw4 (40). The structure of HLA-Cw4 also predicts that proline at P2 would be destabilizing. Substitution of P2Tyr with P2Pro would eliminate the hydrogen bond from the main chain amino group of P2 to the side chain carboxylate oxygen of Glu63 and leave the entire P2 pocket vacant. It is possible that the pool sequencing signal for P2Pro was due to the low levels of HLA-B35 expressed on the surfaces of the cells used for pool sequencing.

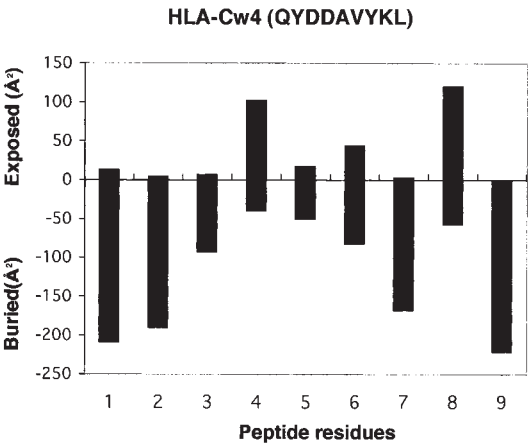


**Figure 4.** Solvent-accessible surface area buried for the peptide. Solvent-accessible surface area buried upon HLA-Cw4 binding is calculated for each residue of the peptide (QYDDAVYKL), using probe radius of 1.4 Å (SURFACE; reference 39).

One of the distinct features of HLA-Cw4 is a P7 pocket located on the side of the α1 helix, formed mostly by residues from the α1 helix (Gln70, Asp74, and Asn77) and the β sheet platform (Ser9, Phe22, Leu95, Arg97, and Phe116). The P7Tyr side chain is secured in the specificity pocket by two hydrogen bonds from the P7Tyr hydroxyl group to the carboxylate oxygen atoms of Asp74. In the known structures of nonameric peptide–MHC complexes, the P5 and P7 side chains are generally oriented toward the α2 helix, whereas the P4 and P6 side chains point toward the α1 helix (32). A well-defined P7 pocket has not been observed in HLA-A and -B structures. In the structure of HLA-E bound to a nonamer derived from the signal peptide of HLA-B8 (47), P7 side chain fills a single pocket down toward the α2 helix, which coincides with the E pocket identified by Saper et al. (41). In HLA-Cw4, the $C_\beta$ atom of the P7Tyr residue points toward the α2 helix; however, the large side chain of Arg156 forces the P7 side chain to turn and point its phenyl ring toward the α1 helix. The P7 pocket in HLA-Cw4 is at the location of the C pocket (41). The presence of Asp9 and Ala73 in the C pocket of some HLA-C alleles has been linked to increased susceptibility to psoriasis vulgaris (48, 49). The distinct features of the C pocket in HLA-Cw4 may also be important in its association with type 2 diabetes (7).

The C pocket in HLA-Cw4 is adjacent to the B pocket

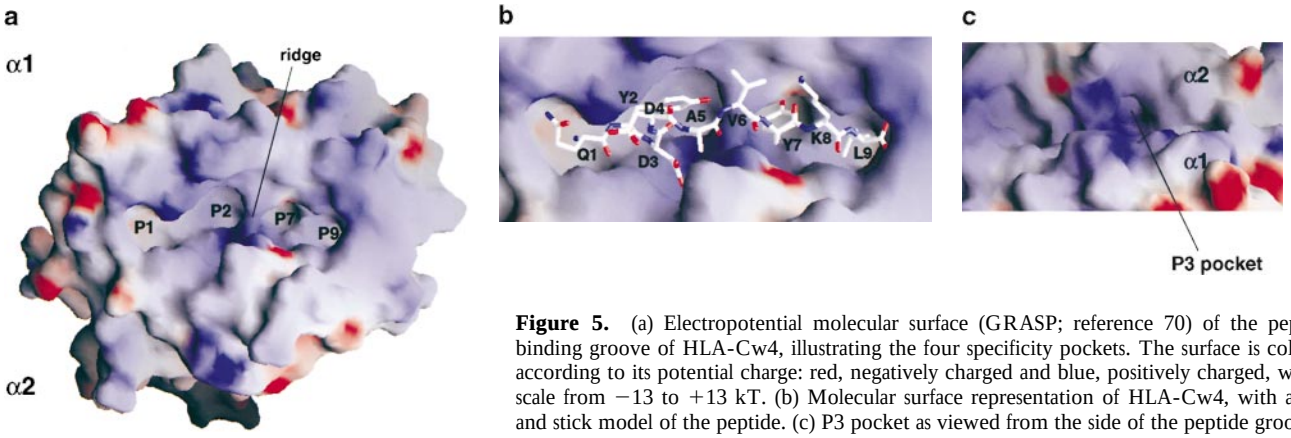


**Figure 5.** (a) Electropotential molecular surface (GRASP; reference 70) of the peptide binding groove of HLA-Cw4, illustrating the four specificity pockets. The surface is colored according to its potential charge: red, negatively charged and blue, positively charged, with a scale from −13 to +13 kT. (b) Molecular surface representation of HLA-Cw4, with a ball and stick model of the peptide. (c) P3 pocket as viewed from the side of the peptide groove.

that hosts the P2 side chain and is separated from the B pocket by a polar ridge formed by the side chains of Ser9, Arg97, and Gln70 (Fig. 5 a). A mouse-specific hydrophobic ridge formed by Trp73, Tyr156, and Trp147 has been found in H-2D$^b$ and H-2L$^d$ (45, 50, 51). A tryptophan wall created by residues Trp97 and Trp114 is located in the middle of the H-2D$^d$ cleft (42).

The P9 pocket at the COOH-terminal end of the peptide binding groove is hydrophobic, formed by the side chains of Leu81, Leu95, Phe116, Tyr123, Ile124, and Trp147. The pocket forms the COOH-terminal boundary of the cleft. The pocket is not completely filled by the side chain of P9Leu. It can host an even larger hydrophobic residue, such as phenylalanine. Hydrophobic PΩ pocket is characteristic of HLA-A2, HLA-E, and all known mouse class I MHC structures (30, 41, 42, 44, 45, 47, 50, 52).

*KIR Binding Site on HLA-Cw4: Electrostatic Interactions Mediate the Binding of KIR2DL1 to HLA-Cw4.* The KIR binding site on HLA-C is located on the α1 domain and includes residues 73, 76, 77, and 80 at the COOH-terminal end of the α1 helix and residue 90 on the loop following it in sequence (14, 53–56). Studies of the KIR3D receptors (e.g., NKB1) that specifically recognize the HLA-Bw4 family indicate that the same region, residues 77–83 in the α1 domain of HLA-B molecules, participates in the interactions with KIR (53, 57). Peptide residues P7 and P8 have also been observed to affect the binding of KIRs to HLA-C and -B molecules (40, 58–60).

In HLA-Cw4, the region surrounding the COOH-terminal end of the α1 helix and residue P8 of the peptide has an electropositive polar surface (Fig. 6 c, blue). The elbow region of KIR2DL1 contains residues involved in HLA-C binding (Met44, Phe45, and Thr70) (18–20, 61); it has an electronegative polar surface (Fig. 6 e, red). The ligand binding site on KIR2DL1 and the receptor binding site on HLA-Cw4 are complementary in their polarity, and recognition of HLA-Cw4 by KIR2DL1 is possibly mediated by the polar interactions between the oppositely charged surfaces on the two molecules.

Among the residues implicated in KIR binding, residue 80 on HLA-C molecules determines the specificity of HLA-Cw4 for KIR2DL1 and, similarly, that of HLA-Cw3 for KIR2DL3 (55). The structure of HLA-Cw4 confirms the importance of residue 80 in mediating the interaction between HLA-C and KIR2D. As shown in Fig. 6 a, the residues that differ between HLA-Cw4 and HLA-Cw3 are concentrated along the peptide binding groove. Once the peptide is bound, however, many of the residues, including residue 77, are buried in their interactions with the peptide (Fig. 6 b). Residue 80 is highly exposed and located at the center of the electropositive surface on HLA-Cw4 that forms the potential KIR binding site (Fig. 6, b and c).

HLA-Cw4 loaded with peptides containing the negatively charged glutamic acid or aspartic acid at P8 are not recognized by a KIR2DL1–Ig fusion protein (40). Peptide residue P8 is important for KIR binding, partly due to the fact that P8 is highly exposed (with 68% of its surface area exposed), with its side chain forming a protrusion on the HLA-Cw4 surface (Fig. 6, b and c). As the P8Lys protrusion is one of the highest points on the HLA-Cw4 surface, it will be readily contacted by KIR2DL1 that approaches HLA-Cw4 from the top of the Cw4 cleft. The positively charged P8Lys in the consensus peptide contributes greatly to the electropositive surface around the COOH-terminal end of the α1 helix. The negatively charged glutamic acid or aspartic acid side chain would result in electronic repulsion between the electronegative surface at the KIR2DL1 elbow and the P8 residue of HLA-Cw4 peptide, thereby abolishing receptor–ligand binding.

A single substitution of tyrosine by glutamic acid at P7 in the peptide also disrupts the interaction between KIR2DL1 and HLA-Cw4 (40). The P7 side chain is buried in a pocket under the α1 helix (compare Figs. 6 a and b). The P7 pocket is acidic, formed in part by the residues Gln70, Asp74, and Asn77. Charge–charge repulsion between the P7Glu side chain and the acidic pocket would destabilize the structure. The effect of the P7 residue on the binding of KIR to HLA-Cw4 is likely to be mediated through the conformational changes of the peptide main chain α1 and α2 helices that are necessary to accommodate the P7 side chain.

The specificity of HLA-Cw4 and KIR2DL1 interaction is also mediated by hydrophobic interactions. As shown by Fig. 6 d, residues that differ between KIR2DL1 and KIR2DL2 form hydrophobic patches adjacent to the electronegative

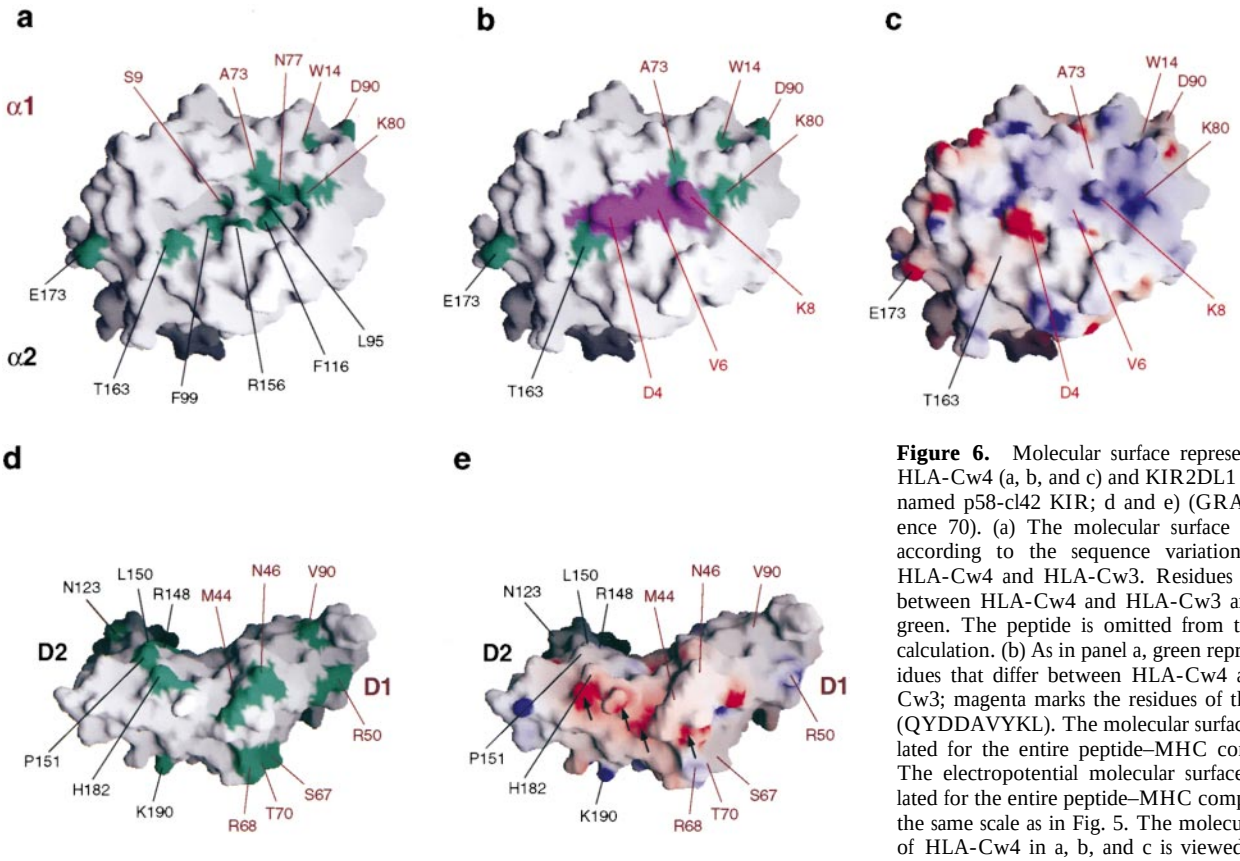


**Figure 6.** Molecular surface representation of HLA-Cw4 (a, b, and c) and KIR2DL1 (originally named p58-cl42 KIR; d and e) (GRASP; reference 70). (a) The molecular surface is colored according to the sequence variation between HLA-Cw4 and HLA-Cw3. Residues that differ between HLA-Cw4 and HLA-Cw3 are colored green. The peptide is omitted from the surface calculation. (b) As in panel a, green represents residues that differ between HLA-Cw4 and HLA-Cw3; magenta marks the residues of the peptide (QYDDAVYKL). The molecular surface is calculated for the entire peptide–MHC complex. (c) The electropotential molecular surface is calculated for the entire peptide–MHC complex, using the same scale as in Fig. 5. The molecular surface of HLA-Cw4 in a, b, and c is viewed from the same orientation in a, b, and c, that is, from the top of the peptide binding groove. Residues from the α1 domain are labeled in brown, whereas those from the α2 domain are labeled in black. Peptide residues are marked in red. (d) The molecular surface is colored according to the sequence variation between KIR2DL1 (specific for HLA-Cw4) and KIR2DL2 (specific for HLA-Cw3). Residues that differ between KIR2DL1 and KIR2DL2 are marked green. (e) The molecular surface is colored according to its potential charge as in c. Arrows point to acidic residues that are located at the domain elbow and form the electronegative polar surface. (These acidic residues include Asp 72, 135, and 183 and Glu187.) The molecular surface of KIR2DL1 is viewed from the same orientation in d and e, that is, facing the domain elbow between D1 and D2. Residues in D1 are labeled in brown, whereas those in D2 are marked black.

surface at the KIR2DL1 elbow (Fig. 6 e). Among these residues, Met44 determines the specificity of KIR2DL1 for HLA-Cw4 (18), and Thr70 affects their binding affinity (20). A single mutation from Met44 in KIR2DL1 to Lys44 found in KIR2DL2 switches the specificity of KIR2DL1 from HLA-Cw4 to HLA-Cw3. Lys44 may disrupt the hydrophobic interactions mediated by Met44. Furthermore, its electropositive side chain may be repelled by the electropositive surface on HLA-Cw4.

## Discussion

The structure of HLA-Cw4 allows us to predict the structural features of the closely related HLA-Cw3 molecule. First, HLA-Cw3 and HLA-Cw4 have different specificities for the P2 pocket. The residues that line the P2 pocket include Ser9 and Phe99 in HLA-Cw4 but Tyr9 and Tyr99 in HLA-Cw3. These large side chains found in HLA-Cw3, if oriented like those in HLA-Cw4, would reduce the size of the P2 pocket and preclude any bulky side chain for the P2 residue. This structural argument is consistent with pool sequencing results, which indicate that the dominant signal for P2 in HLA-Cw3 is alanine (29).

Unlike most known class I MHC structures that possess a P7 pocket coincident with the E pocket under the α2 helix, the HLA-Cw4 structure reveals a P7 pocket on the side of the α1 helix. The P7 pocket in HLA-Cw4 is located in the same area as the C pocket identified by Saper et al. (41). The side chain of P7Tyr in HLA-Cw4 fits into a pocket adjacent to that for P2, partly because the internal hydrogen bonds cause the peptide residues from P4 to P7 to shift toward its $NH_2$ terminus (up to 1.1 Å) and deeper into the cleft (up to 1.6 Å) relative to the Tax peptide bound to HLA-A2. The HLA-Cw3–specific peptides do not contain a P3Asp, which is crucial in forming the internal hydrogen bonds within the HLA-Cw4–bound peptide. Peptides bound to HLA-Cw3 therefore are more likely to adopt conformations similar to those found in HLA-A and -B peptides. In particular, there is not likely to be a shift of the central part of the peptide (P4–P7) toward the peptide $NH_2$ terminus. The large side chain of Arg156 precludes a P7 pocket on the side of the α2 helix in HLA-Cw4. In HLA-Cw3, Arg156 is substituted with the smaller residue Leu156, creating a P7 pocket in the area of the E pocket under the α2 helix. Instead of tyrosine at P7 for HLA-Cw4, pool sequencing indicates that HLA-Cw3 has a strong sig-

nal for phenylalanine or tyrosine at P6. As the residues that form the C pocket are conserved between HLA-Cw4 and HLA-Cw3, it is possible that the C pocket is filled with the aromatic side chain of P6 in HLA-Cw3.

In the structure of the human TCR–HLA-A2 complex (62, 63), two different TCRs contact the entire length of the bound peptide (residues P1, P2, and P4–P8). The sequence and conformation of antigenic peptide determines the specificity of the T cell recognition. In mice, the extensive interaction between the TCR and the peptide across the cleft is observed in the structures of the mouse TCR 2C–H-2K$^b$ and TCR N15–H-2K$^b$ complexes (64–66). Unlike the case with T cells, which are activated by viral antigens presented on class I MHC molecules, recognition of properly processed self class I MHC–peptide assembly by KIR inhibits target cell lysis by NK cells. In mice, Ly-49$^+$ NK cells bind to assembled peptide–class I MHC complexes, but a diverse array of peptides are capable of inducing inhibition (67), indicating that Ly-49 recognition of mouse class I MHC is peptide independent. In humans, both KIR2D and KIR3D contact the COOH-terminal end of the α1 helix (for review see references 9 and 10). Peptides also play a role in the recognition of the HLA-B and -C molecules; peptide residues P7 and P8 appear to affect the binding of KIR to class I MHC molecules directly (40, 58–60). For HLA-Cw4, negatively charged residues at P7 and P8 of the peptide abolish HLA-Cw4–KIR2DL1 binding (40). For HLA-Cw3, two different peptides confer protection of Cw3-bearing target cells from P58.2$^+$ NK cells (68). For HLA-B27, two NK cell clones discriminate among HLA-B27 loaded with four different peptides (59). Therefore, NK cell recognition of class I MHC molecules in humans is peptide dependent but not as specific as T cell recognition, as a much more diverse collection of peptides can confer protection.

The structure of HLA-Cw4 reveals features that may be involved in the recognition of the class I MHC molecule by KIR2DL1. The specific interaction of the receptor–ligand pair appears to involve complementary charged surfaces, with the KIR binding site on HLA-Cw4 being electropositive and the ligand binding site on KIR2DL1 electronegative. Peptide residue P8Lys contributes to specific binding in a unique way in that its side chain is exposed on top of the HLA-Cw4 binding surface, forming a projection that will inevitably be "touched" by the receptor. The structural features of HLA-Cw4 that mediate its interaction with KIR2DL1 may be conserved in the related HLA-C allotypes that are recognized by the same inhibitory NK cell receptor.

We thank L. Mosyak for advice on structure determination, E.O. Long for the cDNA clone of the HLA-Cw4 heavy chain and continuing collaboration on the NK cell receptor, A. Haykov, N. Sinitskaya, and R. Crouse for technical support, D.N. Garboczi, L. Mosyak, Y.H. Ding, and the staff at Cornell High Energy Synchrotron Source (CHESS) for help with data collection, E.O. Long, D.N. Garboczi, J.L. Strominger, and L. Mosyak for critical reading of the manuscript, and H. Huang and R. Gaudet for discussion.

Q.R. Fan is a recipient of a National Science Foundation predoctoral fellowship. D.C. Wiley is an investigator of the Howard Hughes Medical Institute.

Address correspondence to Don C. Wiley, Department of Molecular and Cellular Biology, Howard Hughes Medical Institute, Harvard University, Cambridge, MA 02138. Phone: 617-495-1808; Fax: 617-495-9613; E-mail: dcwadmin@crystal.harvard.edu

Coordinates have been deposited in the Research Collaboratory for Structural Bioinformatics (RCSB) with the RCSB ID 009143 and Protein Data Bank accession code 1QQD. Coordinates are available before their release by e-mail (fan@xtal200.harvard.edu).

*Submitted: 1 February 1999 Revised: 7 April 1999 Accepted: 11 May 1999*

## References

1. Madden, D.R. 1995. The three-dimensional structure of peptide-MHC complexes. *Annu. Rev. Immunol.* 13:587–622.
2. Stern, L.J., and D.C. Wiley. 1994. Antigenic peptide binding by class I and class II histocompatibility proteins. *Structure*. 94: 1–10.
3. Zemmour, J., and P. Parham. 1992. Distinctive polymorphism at the HLA-C locus: implications for the expression of HLA-C. *J. Exp. Med.* 176:937–950.
4. Johnson, R.P., A. Trocha, T.M. Buchanan, and B.D. Walker. 1993. Recognition of a highly conserved region of human immunodeficiency virus type 1 gp120 by an HLA-Cw4-restricted cytotoxic T-lymphocyte clone. *J. Virol.* 67:438–445.
5. Littaua, R.A., M.B.A. Oldstone, A. Takeda, C. Debouck, J.T. Wong, C.U. Tuazon, B. Moss, F. Kievitz, and F.A. Ennis. 1991. An HLA-C-restricted CD8$^+$ cytotoxic T-lymphocyte clone recognizes a highly conserved epitope on human immunodeficiency virus type 1 gag. *J. Virol.* 65:4051–4056.
6. Neisig, A., C.J.M. Melief, and J. Neefjes. 1998. Reduced cell surface expression of HLA-C molecules correlates with restricted peptide binding and stable TAP interaction. *J. Immunol.* 160:171–179.
7. Groop, L., S. Koskimies, R. Pelkonen, and E.-M. Tolppanen. 1983. Increased frequency of HLA-Cw4 in type 2 diabetes. *Acta. Endocrinol.* 104:375–378.
8. Carrington, M., G.W. Nelson, M.P. Martin, T. Kissner, D. Vlahov, J.J. Goedert, R. Kaslow, S. Buchbinder, K. Hoots,

and S.J. O'Brien. 1999. HLA and HIV-1: heterozygote advantage and B*35-Cw*04 disadvantage. *Science*. 283:1748–1752.
9. Long, E.O., and N. Wagtmann. 1997. Natural killer cell receptors. *Curr. Opin. Immunol.* 9:344–350.
10. Lanier, L.L. 1998. NK cell receptors. *Annu. Rev. Immunol.* 16:359–393.
11. Wagtmann, N., S. Rajagopalan, C.C. Winter, M. Peruzzi, and E.O. Long. 1995. Killer cell inhibitory receptors specific for HLA-C and HLA-B identified by direct binding and by functional transfer. *Immunity*. 3:801–809.
12. Colonna, M., and J. Samaridis. 1995. Cloning of Ig-superfamily members associated with HLA-C and HLA-B recognition by human NK cells. *Science*. 268:405–408.
13. D'Andrea, A., C. Chang, K. Franz-Bacon, T. McClanahan, J.H. Phillips, and L.L. Lanier. 1995. Molecular cloning of NKB1. A natural killer cell receptor for HLA-B allotypes. *J. Immunol*. 155:2306–2310.
14. Colonna, M., G. Borsellino, M. Falco, G.B. Ferrara, and J.L. Strominger. 1993. HLA-C is the inhibitory ligand that determines dominant resistance to lysis by NK1- and NK2-specific natural killer cells. *Proc. Natl. Acad. Sci. USA*. 90:12000–12004.
15. Moretta, A., M. Vitale, C. Bottino, A.M. Orengo, L. Morelli, R. Augugliaro, M. Barbaresi, E. Ciccone, and L. Moretta. 1993. p58 molecules as putative receptors for major histocompatibility complex (MHC) class I molecules in human natural killer (NK) cells: anti-p58 antibodies reconstitute lysis of MHC class I–protected cells in NK clones displaying different specificities. *J. Exp. Med.* 178:597–604.
16. Lanier, L.L., J.E. Gumperz, P. Parham, I. Melero, M. Lopez-Botet, and J.H. Phillips. 1995. The NKB1 and HP-3E4 NK cell receptors are structurally distinct glycoproteins and independently recognize polymorphic HLA-B and HLA-C molecules. *J. Immunol*. 154:3320–3327.
17. Fan, Q.R., L. Mosyak, C.C. Winter, N. Wagtmann, E.O. Long, and D.C. Wiley. 1997. Structure of the inhibitory receptor for human natural killer cells resembles haematopoietic receptors. *Nature*. 389:96–100.
18. Winter, C.C., and E.O. Long. 1997. A single amino acid in the p58 killer cell inhibitory receptor controls the ability of natural killer cells to discriminate between the two groups of HLA-C allotypes. *J. Immunol*. 158:4026–4028.
19. Winter, C.C., J.E. Gumperz, P. Parham, E.O. Long, and N. Wagtmann. 1998. Direct binding and functional transfer of NK cell inhibitory receptors reveal novel patterns of HLA-C allotype recognition. *J. Immunol*. 161:571–577.
20. Biassoni, R., A. Pessino, A. Malaspina, C. Cantoni, C. Bottino, S. Sivori, L. Moretta, and A. Moretta. 1997. Role of amino acid position 70 in the binding affinity of p50.1 and p58.1 receptors for HLA-Cw4 molecules. *Eur. J. Immunol.* 27:3095–3099.
21. Fan, Q.R., D.N. Garboczi, C.C. Winter, N. Wagtmann, E.O. Long, and D.C. Wiley. 1996. Direct binding of a soluble natural killer cell inhibitory receptor to a soluble human leukocyte antigen-Cw4 class I major histocompatibility complex molecule. *Proc. Natl. Acad. Sci. USA*. 93:7178–7183.
22. Garboczi, D.N., D.T. Hung, and D.C. Wiley. 1992. HLA-A2-peptide complexes: refolding and crystallization of molecules expressed in *Escherichia coli* and complexed with single antigenic peptides. *Proc. Natl. Acad. Sci. USA*. 89:3429–3433.
23. Nevaza, Z. 1994. AMoRE-an automated package for molecular replacement. *Acta. Crystallogr*. A50:157–163.
24. Madden, D.R., J.C. Gorga, J.L. Strominger, and D.C. Wiley. 1992. The three-dimensional structure of HLA-B27 at 2.1 Å resolution suggests a general mechanism for tight peptide binding to MHC. *Cell*. 70:1035–1048.
25. Brünger, A.T. 1992. X-PLOR Version 3.1.Å System for X-ray Crystallography and NMR. Yale University Press, New Haven, CT.
26. Jones, T.A. 1985. Diffraction methods for biological macromolecules: interactive computer graphics. *FRODO*. 115: 157–171.
27. Brünger, A.T., P.D. Adams, G.M. Clore, W.L. Delano, P. Gros, R.W. Grosse-Kunstleve, J.S. Jiang, J. Kuszewski, M. Nilges, N.S. Pannu, et al. 1998. Crystallography and NMR system: a new software suite for macromolecular structure determination. *Acta. Crystallogr*. D54:905–921.
28. Sidney, J., M.-F. del Guercio, S. Southwood, V.H. Engelhard, E. Appella, H.-G. Rammensee, K. Falk, O. Rotzschke, M. Takiguchi, R.T. Kubo, et al. 1995. Several HLA alleles share overlapping peptide specificities. *J. Immunol.* 154:247–259.
29. Falk, K., O. Rotzschke, B. Grahovac, D. Schendel, S. Stevanovic, V. Gnau, G. Jung, J.L. Strominger, and H.-G. Rammensee. 1993. Allele-specific peptide ligand motifs of HLA-C molecules. *Proc. Natl. Acad. Sci. USA*. 90:12005–12009.
30. Bjorkman, P.J., M.A. Saper, B. Samraoui, W.S. Bennett, J.L. Strominger, and D.C. Wiley. 1987. Structure of the human class I histocompatibility antigen HLA-A2. *Nature.* 329: 506–512.
31. Garrett, P.J., M.A. Saper, P.J. Bjorkman, J.L. Strominger, and D.C. Wiley. 1989. Specificity pockets for the side chains of peptide antigens in HLA-Aw68. *Nature*. 342:692–696.
32. Madden, D.R., D.N. Garboczi, and D.C. Wiley. 1993. The antigenic identity of peptide-MHC complexes: a comparison of the conformations of five viral peptides presented by HLA-A2. *Cell.* 75:693–708.
33. Smith, K.J., S.W. Reid, K. Harlos, A.J. McMichael, D.I. Stuart, J.I. Bel, and E.Y. Jones. 1996. Bound water structure and polymorphic amino acids act together to allow the binding of different peptides to MHC class I HLA-B53. *Immunity.* 4:215–228.
34. Smith, K.J., S.W. Reid, D.I. Stuart, A.J. McMichael, E.Y. Jones, and J.I. Bell. 1996. An altered position of the α2 helix of MHC class I is revealed by the crystal structure of HLA-B*3501. *Immunity*. 4:203–213.
35. Sundbäck, J., M.C. Nakamura, M. Waldenström, E.C. Niemi, W.E. Seaman, J.C. Ryan, and K. Kärre. 1998. The α2 domain of H-2D$^d$ restricts the allelic specificity of the murine NK cell inhibitory receptor Ly-49A. *J. Immunol.* 160:5971–5978.
36. Karlhofer, F.M., R.K. Ribaudo, and W.M. Yokoyama. 1992. MHC class I alloantigen specificity of Ly-49$^+$ IL-2 activated natural killer cells. *Nature.* 358:66–70.
37. Orihuela, M., D.H. Margulies, and W.M. Yokoyama. 1996. The natural killer cell receptor Ly-49A recognizes a peptide-induced conformational determinant on its major histocompatibility complex class I ligand. *Proc. Natl. Acad. Sci. USA*. 93:11792–11797.
38. Gao, G.F., J. Tormo, U.C. Gerth, J.R. Wyer, A.J. McMichael, D.I. Stuart, J.I. Bell, E.Y. Jones, and B.K. Jakobsen. 1997. Crystal structure of the complex between human CD8α and HLA-A2. *Nature.* 387:630–634.
39. 1994. Collaborative computational project number 4. The CCP4 suite: programs for protein crystallography. *Acta. Crystallogr.* D50:760–776.
40. Rajagopalan, S., and E.O. Long. 1997. The direct binding of a p58 killer cell inhibitory receptor to human histocompatibility leukocyte antigen (HLA)-Cw4 exhibits peptide selectivity. *J. Exp. Med.* 185:1523–1528.
41. Saper, M.A., P.J. Bjorkman, and D.C. Wiley. 1991. Refined

structure of the human histocompatibility antigen HLA-A2 at 2.6 Å resolution. *J. Mol. Biol.* 219:277–319.
42. Achour, A., K. Persson, R.A. Harris, J. Sundback, C.L. Sentman, Y. Lindqvist, G. Schneider, and K. Karre. 1998. The crystal structure of H-2D$^d$ MHC class I complexed with the HIV-1-derived peptide P18-I10 at 2.4 Å resolution: implications for T cell and NK cell recognition. *Immunity*. 9:199–208.
43. Li, H., K. Natarajan, E.L. Malchiodi, D.H. Margulies, and R.A. Mariuzza. 1998. Three-dimensional structure of H-2D$^d$ complexed with an immunodominant peptide from human immunodeficiency virus envelope glycoprotein 120. *J. Mol. Biol.* 283:179–191.
44. Fremont, D.H., M. Matsumura, E.A. Stura, P.A. Peterson, and I.A. Wilson. 1992. Crystal structures of two viral peptides in complex with murine MHC class I H-2K$^b$. *Science*. 257:919–927.
45. Young, A.C.M., W. Zhang, J.C. Sacchettini, and S.G. Nathenson. 1994. The three-dimensional structure of H-2D$^b$ at 2.4. Å resolution: implications for antigen-determinant selection. *Cell*. 76:39–50.
46. Wang, C.-R., A.R. Castano, P.A. Peterson, C. Slaughter, K.F. Lindahl, and J. Deisenhofer. 1995. Nonclassical binding of formylated peptide in crystal structure of the MHC class Ib molecule H2–M3. *Cell*. 82:655–664.
47. O'Callaghan, C.A., J. Tormo, B.E. Willcox, V.M. Braud, B.K. Jakobsen, D.I. Stuart, A.J. McMichael, J.I. Bell, and E.Y. Jones. 1998. Structural features impose tight peptide binding specificity in the nonclassical MHC molecule HLA-E. *Mol. Cell*. 1:531–541.
48. Asahina, A., S. Akazaki, S. Nakagawa, S. Kuwata, K. Tokunaga, Y. Ishibashi, and T. Juji. 1991. Specific nucleotide sequence of HLA-C is strongly associated with psoriasis vulgaris. *J. Invest. Dermatol*. 97:254–258.
49. Asahina, A., S. Kuwata, K. Tokunaga, T. Juji, and H. Nakagawa. 1996. Study of aspartate at residue 9 of HLA-C molecules in Japanese patients with psoriasis vulgaris. *J. Dermatol. Sci*. 13:125–133.
50. Balendiran, G.K., J.C. Solheim, A.C. Young, T.H. Hansen, S.G. Nathenson, and J.C. Sacchettini. 1997. The three-dimensional structure of an H-2L$^d$-peptide complex explains the unique interaction of L$^d$ with β2 microglobulin and peptide. *Proc. Natl. Acad. Sci. USA*. 94:6880–6885.
51. Speir, J.A., K.C. Garcia, A. Brunmark, M. Degano, P.A. Peterson, L. Teyton, and I.A. Wilson. 1998. Structural basis of 2C TCR allorecognition of H-2L$^d$ peptide complexes. *Immunity*. 8:553–562.
52. Zhang, W.G., A.C.M. Young, M. Imarai, S.G. Nathenson, and J.C. Sacchettini. 1992. Crystal structure of the major histocompatibility complex class I H-2K$^b$ molecule containing a single viral peptide: implications for peptide binding and T-cell receptor recognition. *Proc. Natl. Acad. Sci. USA*. 89:8403–8407.
53. Cella, M., A. Longo, G.B. Ferrara, J.L. Strominger, and M. Colonna. 1994. NK3-specific natural killer cells are selectively inhibited by Bw4-positive HLA alleles with isoleucine 80. *J. Exp. Med*. 180:1235–1242.
54. Biassoni, R., M. Falco, A. Cambiaggi, P. Costa, S. Verdiani, D. Pende, R. Conte, C. DiDonato, P. Parham, and L. Moretta. 1995. Single amino acid substitutions can influence the NK-mediated recognition of HLA-C molecules: role of serine-77 and lysine-80 in the target cell protection from lysis mediated by "group 2" or "group 1" NK clones. *J. Exp. Med*. 182:605–610.
55. Mandelboim, O., H.T. Reyburn, M. Vales-Gomez, L. Pazmany, M. Colonna, G. Borsellino, and J.L. Strominger. 1996. Protection from lysis by natural killer cells of group 1 and 2 specificity is mediated by residue 80 in human histocompatibility leukocyte antigen C alleles and also occurs with empty major histocompatibility complex molecules. *J. Exp. Med*. 184:913–922.
56. Mandelboim, O., H.T. Reyburn, E.G. Sheu, M. Vales-Gomez, D.M. Davis, B. Wilson, L. Pazmany, and J.L. Strominger. 1997. The binding site of NK receptors on HLA-C molecules. *Immunity*. 6:341–350.
57. Gumperz, J.E., V. Litwin, J.H. Phillips, L.L. Lanier, and P. Parham. 1995. The Bw4 public epitope of HLA-B molecules confers reactivity with NK cell clones that express NKB1, a putative HLA receptor. *J. Exp. Med*. 181:113–114.
58. Malnati, M.S., M. Peruzzi, K.C. Parker, W.E. Biddison, E. Ciccone, A. Moretta, and E.O. Long. 1995. Peptide specificity in the recognition of MHC class I by natural killer cell clones. *Science*. 267:1016–1018.
59. Peruzzi, M., K.C. Parker, E.O. Long, and M.S. Malnati. 1996. Peptide sequence requirements for the recognition of HLA-B*2705 by specific natural killer cells. *J. Immunol*. 157: 3350–3356.
60. Mandelboim, O., S.B. Wilson, M. Valés-Gómez, H.T. Reyburn, and J.L. Strominger. 1997. Self and viral peptides can initiate lysis by autologous natural killer cells. *Proc. Natl. Acad. Sci. USA*. 94:4604–4609.
61. Valés-Gómez, M., H.T. Reyburn, R.A. Erskine, and J.L. Strominger. 1998. Differential binding to HLA-C of p50-activating and p58-inhibitory natural killer cell receptors. *Proc. Natl. Acad. Sci. USA*. 95:14326–14331.
62. Garboczi, D.N., P. Ghosh, U. Utz, Q.R. Fan, W.E. Biddison, and D.C. Wiley. 1996. Structure of the complex between human T-cell receptor, viral peptide and HLA-A2. *Nature*. 384:134–141.
63. Ding, Y.-H., K.J. Smith, D.N. Garboczi, U. Utz, W.E. Biddison, and D.C. Wiley. 1998. Two human T cell receptors bind in a similar diagonal mode to the HLA-A2/tax peptide complex using different TCR amino acids. *Immunity*. 8:403–411.
64. Garcia, K.C., M. Degano, R.L. Stanfield, A. Brunmark, M.R. Jackson, P.A. Peterson, L. Teyton, and I.A. Wilson. 1996. Structure of an αβ T cell receptor at 2.5 Å and its orientation in the TCR-MHC complex. *Science*. 274:209–219.
65. Garcia, K.C., M. Degano, L.R. Pease, M. Huang, P.A. Peterson, L. Teyton, and I.A. Wilson. 1998. Structural basis of plasticity in T cell receptor recognition of a self peptide-MHC antigen. *Science*. 279:1166–1172.
66. Teng, M.K., A. Smolyar, A.G. Tse, J.H. Liu, J. Liu, R.E. Hussey, S.G. Nathenson, H.C. Chang, E.L. Reinherz, and J.H. Wang. 1998. Identification of a common docking topology with a substantial variation among different TCR-peptide-MHC complexes. *Curr. Biol.* 8:409–412.
67. Correa, I., and D.H. Raulet. 1995. Binding of diverse peptides to MHC class I molecules inhibits target cell lysis by activated natural killer cells. *Immunity*. 2:61–71.
68. Zappacosta, F., F. Borrego, A.G. Brooks, K.C. Parker, and J.E. Coligan. 1997. Peptides isolated from HLA-Cw*0304 confer different degrees of protection from natural killer cell-mediated lysis. *Proc. Natl. Acad. Sci. USA*. 94:6313–6318.
69. Carson, M. 1987. Ribbon models of macromolecules. *J. Mol. Graph.* 5:103–106.
70. Nicholls, A., K.A. Sharp, and B. Honig. 1991. Protein folding and association: insights from the interfacial and thermodynamic properties of hydrocarbons. *Proteins*. 11:281–296.